

Southern Illinois University Carbondale OpenSIUC

Publications

Department of Physics

5-7-2012

The Comparison of Direct and Indirect Methods for Determining the Magnetocaloric Parameters in the Heusler Alloy Ni₅₀Mn_{34.8}In_{14.2}B

Igor Dubenko

Southern Illinois University Carbondale

Tampas Samanta

Southern Illinois University Carbondale

Abdiel Quetz

Southern Illinois University Carbondale

Alexander Kazakov

Moscow State University

Igor Rodionov

Moscow State University

See next page for additional authors

Follow this and additional works at: http://opensiuc.lib.siu.edu/phys_pubs

© 2012 American Institute of Physics

Published in *Applied Physics Letters*, Vol. 100 No. 19 (2012) at doi: [10.1063/1.4714539](https://doi.org/10.1063/1.4714539)

Recommended Citation

Dubenko, Igor, Samanta, Tampas, Quetz, Abdiel, Kazakov, Alexander, Rodionov, Igor, Mettus, Dennis, Prudnikov, Valerii, Stadler, Shane, Adams, Philip W., Prestigiacomo, Joseph, Granovsky, Alexander B., Zhukov, Arcady and Ali, Naushad. "The Comparison of Direct and Indirect Methods for Determining the Magnetocaloric Parameters in the Heusler Alloy Ni₅₀Mn_{34.8}In_{14.2}B." (May 2012).

This Article is brought to you for free and open access by the Department of Physics at OpenSIUC. It has been accepted for inclusion in Publications by an authorized administrator of OpenSIUC. For more information, please contact opensiuc@lib.siu.edu.

Authors

Igor Dubenko, Tampas Samanta, Abdiel Quetz, Alexander Kazakov, Igor Rodionov, Dennis Mettus, Valerii Prudnikov, Shane Stadler, Philip W. Adams, Joseph Prestigiacomo, Alexander B. Granovsky, Arcady Zhukov, and Naushad Ali

The comparison of direct and indirect methods for determining the magnetocaloric parameters in the Heusler alloy $\text{Ni}_{50}\text{Mn}_{34.8}\text{In}_{14.2}\text{B}$

Igor Dubenko,¹ Tapas Samanta,¹ Abdiel Quetz,¹ Alexander Kazakov,² Igor Rodionov,² Denis Mettus,² Valerii Prudnikov,² Shane Stadler,³ Philip Adams,³ Joseph Prestigiacomo,³ Alexander Granovsky,^{2,4,5} Arcady Zhukov,^{4,5} and Naushad Ali¹

¹*Department of Physics, Southern Illinois University, Carbondale, Illinois 62901, USA*

²*Faculty of Physics, Moscow State University, Vorob'evy Gory, 119991 Moscow, Russia*

³*Department of Physics & Astronomy, Louisiana State University, Baton Rouge, Louisiana 70803, USA*

⁴*IKERBASQUE, The Basque Foundation for Science, 48011 Bilbao, Spain*

⁵*Departamento de Física de Materiales, Facultad de Química, Universidad del País Vasco, Paseo M. de Lardizabal 3, 20018 Donostia—San Sebastián, Spain*

(Received 26 February 2012; accepted 25 April 2012; published online 7 May 2012)

The magnetocaloric properties of the $\text{Ni}_{50}\text{Mn}_{34.8}\text{In}_{14.2}\text{B}$ Heusler alloy have been studied by direct measurements of the adiabatic temperature change ($\Delta T_{\text{AD}}(T, H)$) and indirectly by magnetization ($M(T, H)$), differential scanning calorimetry, and specific heat ($C(T, H)$) measurements. The presence of a first-order ferromagnetic-paramagnetic transition has been detected for $\text{Ni}_{50}\text{Mn}_{34.8}\text{In}_{14.2}\text{B}$ at 320 K. The magnetocaloric parameters, i.e., the magnetic entropy change ($\Delta S_{\text{M}} = (2.9\text{--}3.2)$ J/kgK) and the adiabatic temperature change ($\Delta T_{\text{AD}} = (1.3\text{--}1.52)$ K), have been evaluated for $\Delta H = 1.8$ T from $C_{\text{p}}(T, H)$ and $M(T, H)$ data and from direct $\Delta T_{\text{AD}}(T, H)$ measurements. The extracted magnetocaloric parameters are comparable to those of Gd. © 2012 American Institute of Physics. [<http://dx.doi.org/10.1063/1.4714539>]

The off-stoichiometric Ni-Mn-In based Heusler alloys that undergo a magnetostructural first order transformation (MST) near room temperature constitute a class of magnetic materials that is important for both fundamental research and applications, due to their wide diversity of physical properties and corresponding underlying physics. These compounds are characterized by inhomogeneous structural and magnetic phases that result in significant magnetoresponse properties, such as “normal” and “inverse” magnetocaloric effects (MCE),^{1–5} magnetoresistance,^{6,7} Hall effects,⁸ and exchange bias.⁹ Such behaviors make these compounds attractive for multifunctional applications in microelectronics and magnetic refrigerators. In many cases, the mechanisms that are responsible for the properties related to the MST are still far from being well understood. Moreover, these properties and the characteristic temperatures, such as the temperature of the transition from the high-temperature austenitic phase to the low-temperature martensitic phase (T_{A}) and of the corresponding reverse transition (T_{M}), and the Curie temperatures of austenitic (T_{C}) and martensitic (T_{CM}) states, are sensitive to elemental substitution and stoichiometric variation in ways that are difficult to predict. Therefore, it is highly desirable to search for and study new materials that exhibit magnetostructural transitions.

Several magnetic phases have been observed in the austenitic and martensitic states of Ni-Mn-In Heusler alloys, namely, ferromagnetic ($T < T_{\text{CM}}$) and low magnetization (paramagnetic or antiferromagnetic) states ($T_{\text{CM}} < T < T_{\text{M}}$) in the martensitic phase, and ferromagnetic ($T < T_{\text{C}}$) and paramagnetic states ($T > T_{\text{C}}$) in the austenitic phase. It has been shown that, as a rule, the MST occurs from a low magnetization martensitic state to a ferromagnetic austenitic state, resulting in the large jump in magnetization that is a main requirement for large MCE.^{1–5,9} Since, for a MST, the total change in entropy (ΔS_{T}) is due to both the magnetic

entropy change (ΔS_{M}) and the entropy difference between two crystallographic modifications (ΔS_{C}), the MCE properties at the MST are much more complicated than at T_{C} .

In the present work, the MCE parameters at the MST between the ferromagnetic martensite to paramagnetic austenite phase of $\text{Ni}_{50}\text{Mn}_{34.8}\text{In}_{14.2}\text{B}$ have been investigated by different methods based on measurements of thermomagnetic curves $M(T, H)$, specific heat $C(T, H)$, and direct adiabatic temperature changes ΔT_{AD} . Substituting B for In in $\text{Ni}_{50}\text{Mn}_{34.8}\text{In}_{14.2}\text{B}$ induced a large shift of both T_{CM} and (T_{A} , T_{M}) above T_{C} , providing the transition from the paramagnetic austenitic phase to the ferromagnetic martensitic phase and the jump in magnetization at T_{M} that favors large MCE.

The samples were fabricated by conventional arc-melting in a high-purity argon atmosphere using 4N purity elements and were annealed in high vacuum ($\approx 10^{-4}$ Torr) for 24 h at 850 °C. The phase purity of the samples has been confirmed by x-ray powder diffraction at room temperature using $\text{CuK}\alpha$ radiation. Thermomagnetic curves $M(H, T)$ have been studied using a vibrating sample magnetometer (Lake Shore VSM 7400 System) and a superconducting quantum interference device (SQUID) magnetometer (by Quantum Design, USA) in a temperature interval of 80–400 K, and in fields up to 1.8 T. Direct measurements of ΔT_{AD} under an applied magnetic field (FC) have been done using an adiabatic magnetocalorimeter (MagEq MMS 801) in a temperature range of 250–350 K and in magnetic fields up to 1.8 T. The external magnetic fields have been ramped at a rate of up to 2.0 T/s during ΔT_{AD} measurements. Heat capacity measurements were done using a physical properties measurement system (PPMS by Quantum Design, INC.) using a vertical puck arrangement, in a temperature range of 275–380 K and in fields up to 5.0 T. The differential scanning calorimetry (DSC) measurements were carried out employing a DSC 8000 (with the ramp rate of 20 K/min during heating

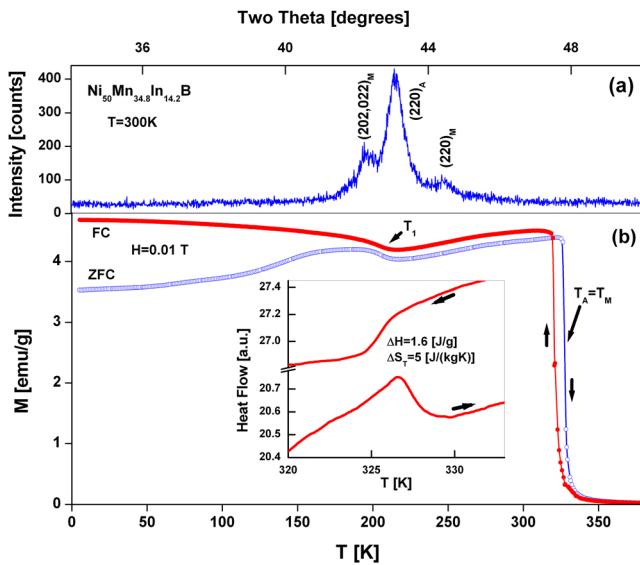


FIG. 1. (a) XRD pattern of $\text{Ni}_{50}\text{Mn}_{34.8}\text{In}_{14.2}\text{B}$ obtained at 300 K using $\text{CuK}\alpha$ radiation. Indexes “A” and “M” identify the XRD peaks from the cubic austenitic and tetragonal martensitic phases, respectively; (b) the temperature dependencies of the magnetization obtained at 0.01 T after the sample was cooled from 380 to 5 K at zero field (ZFC), and after cooling in the presence of a FC. Arrows indicate the transition temperatures. Inset: temperature dependencies of the heat flow of $\text{Ni}_{50}\text{Mn}_{35}\text{In}_{14}\text{B}$. Arrows indicate the direction of temperature changes.

and cooling) in the temperature range of 103–573 K. The latent heat (L) has been estimated from the measured endothermic peak of the heat flow curve of the DSC measurement using: $L = \int_{T_s}^{T_f} \frac{dQ}{dT} dT$, where $\frac{dQ}{dT}$ is the change in heat flow with respect to temperature, and T_s and T_f are the start and final temperatures, respectively, of the MST on heating.

The room temperature XRD pattern clearly indicates that $\text{Ni}_{50}\text{Mn}_{34.8}\text{In}_{14.2}\text{B}$ is composed of austenitic and martensitic phases at room temperature (see Fig. 1(a)). The relatively sharp change in magnetization at $T_A \approx 320$ K is associated with a first order phase transition from the paramagnetic austenitic phase to a ferromagnetic martensitic phase (shown in Fig. 1(b)). In fact, in these alloys, there is no ferromagnetic austenite and low magnetization martensite, which is a unique feature of the Ni-Mn-In-Z alloys. The difference between the ZFC and FC $M(T)$ curves in the low-temperature region ($T < T_1$) are typical of many Ni-Mn-In based compounds and is related to the magnetic heterogeneity that results in exchange bias effects.⁵ A slight increase in magnetization was observed in the temperature interval $T_1 < T < T_C$. The first order nature of the phase transition at T_C was also confirmed by the relatively large endothermic/exothermic peaks and temperature hysteresis of the heat flow during heating/cooling cycles (shown in the inset Fig. 1). The ferromagnetic character of the magnetic order below $T_C \sim T_A$ was also verified by thermomagnetic curves $M(H, T)$, as shown in Figs. 2 and 3. The substitution of B for In eliminates the low magnetization state of the parent compound and results in the stabilization of the ferromagnetic martensitic phase in terms of the temperature and also results in ferromagnetic martensite to paramagnetic austenite phase transition at T_M .

The role of boron in the martensitic transformation of Heusler alloys had been studied by partially introducing boron

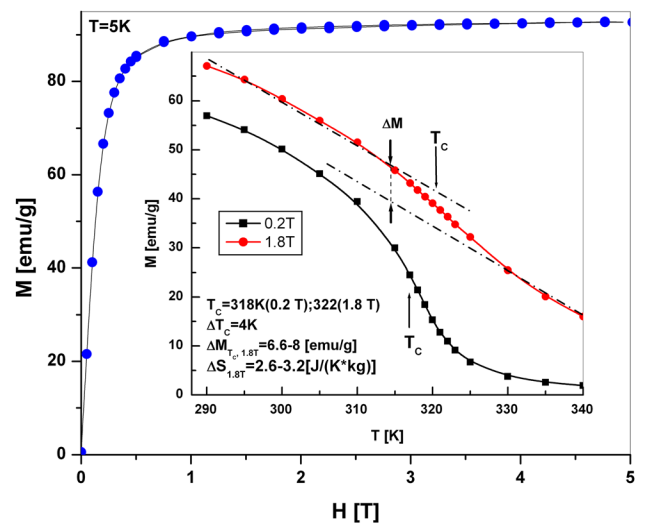


FIG. 2. Magnetization curves, $M(H)$, of $\text{Ni}_{50}\text{Mn}_{34.8}\text{In}_{14.2}\text{B}$ at $T = 5$ K. Inset: Temperature dependencies of magnetization for applied fields $H = 0.01$ and 1.8 T. Arrows indicate T_C , determined as the inflection point of $M(T)$ at different applied fields, and the change in magnetization ΔM at the MST.

in the lattice sites in $\text{Ni}_2\text{Mn}(\text{GaB})$ ¹⁰ and $\text{Ni}_{50}\text{Mn}_{36.5}(\text{Sb}, \text{B})$ ¹¹ and for B in the interstitial sites of the crystal cell in the case of $\text{Ni}_{43}\text{Mn}_{46}\text{Sn}_{11}$.¹² An increase in T_M has been reported for these three systems and influence of the change in interatomic distance (crystal cell parameters) on T_M has been discussed. It has been shown that the substitution of B for Ga and Sb results in a contraction of the lattice cell,^{10,11} while interstitial boron atoms in $\text{Ni}_{43}\text{Mn}_{46}\text{Sn}_{11}$ expand the lattice cell.¹² Therefore, change in interatomic distance induced by B is not a major factor responsible for the increase of the temperature of the martensitic transformation in these alloys.

Recently, an important role of the Ni-Mn electron hybridization for the martensitic transformation in Mn-rich Ni-Mn-X alloys was revealed through hard-x-ray photoelectron spectroscopy measurements and *ab initio* calculations.¹⁴ It is well known that the electron hybridization is mainly determined by the local atomic order. The local atomic surroundings of the atoms in the parent Heusler alloys are

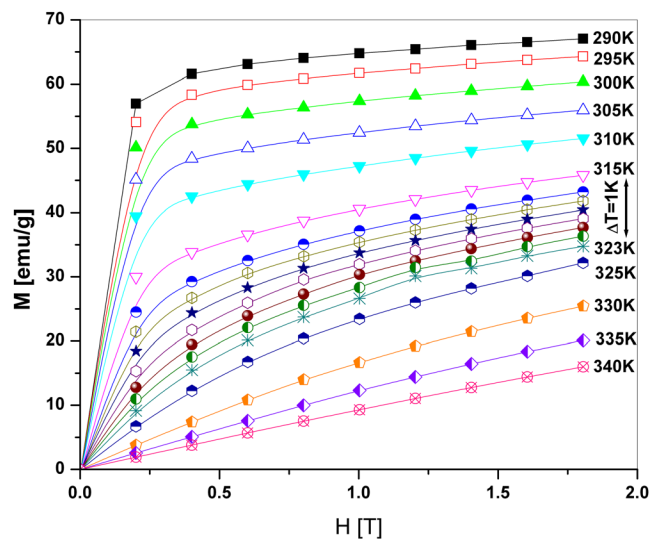


FIG. 3. Isothermal magnetization curves of $\text{Ni}_{50}\text{Mn}_{34.8}\text{In}_{14.2}\text{B}$ for different temperatures in the vicinity of the magnetostructural transition.

modified by boron in both interstitial positions and in “regular” (Sb or In) sites. Moreover, in the latter case, the large differences in metallic radii (R) of B ($R = 0.098$ nm) and In or Sb ($R = 0.1663$ or 0.159 nm)¹³ also favor changes in electronic structure and can result in a change of the martensitic transition temperatures. Thus, the observed increase in T_M is most likely due to the change in 3d hybridization in $\text{Ni}_{50}\text{Mn}_{34.8}\text{In}_{14.2}\text{B}$ relative to that of the parent alloy. However, the detailed mechanisms of the influence of the B atoms on the martensitic temperatures is not clear and worthy for future investigation.

The results of the studies of the specific heat capacity $C(T,H)$ and direct measurements of the adiabatic temperature change (ΔT_{AD}) of $\text{Ni}_{50}\text{Mn}_{34.8}\text{In}_{14.2}\text{B}$ are shown in Fig. 4. The heat capacity at zero applied magnetic field shows a λ -type anomaly in the vicinity of T_C , typical for temperature-induced, first order transitions. Application of a magnetic field suppresses the maximum of $C(T,H)$ and shifts it to higher temperature. Such behavior of $C(T,H)$ is expected in the vicinity of T_C and confirms the results of the magnetization studies. The $\Delta T_{AD}(T)$ curve shows a maximum value of about 1.4 K in the vicinity of the MST temperature at a magnetic field of 1.8 T and about 1 K for $\Delta H = 1$ T (not shown). The change in the adiabatic temperature at the MST is comparable to that observed for $\text{Ni}_{50}\text{Mn}_{35}\text{In}_{14}\text{X}$ ($X = \text{In}, \text{Al}$, and Ge).¹⁵

Let us now compare the values of ΔT_{AD} and ΔS obtained by the different methods. Using DSC measurements, we found that the latent heat at the transition is about $L \approx 1.6$ J/g, corresponding to a total entropy change of $\Delta S_T = 5$ J/kg K. This value is quite reasonable and is of the same order of magnitude as $\Delta S_T = 7$ J/kg K as observed for the transformation between the monoclinic and orthorhombic states in $\text{Gd}_5(\text{Si}_2\text{Ge}_2)$.¹⁶ $\Delta S_M(H)$ can be estimated from $M(T,H)$ curves (see Figures 2 and 3) using a common numerical recipe from a Maxwell relation from the Clausius-Clapeyron equation and from the $C(T,H)$ curves using $S(T,H)_H = \int_0^T \frac{C(T,H)_H}{T} dT$ and the isothermal entropy change

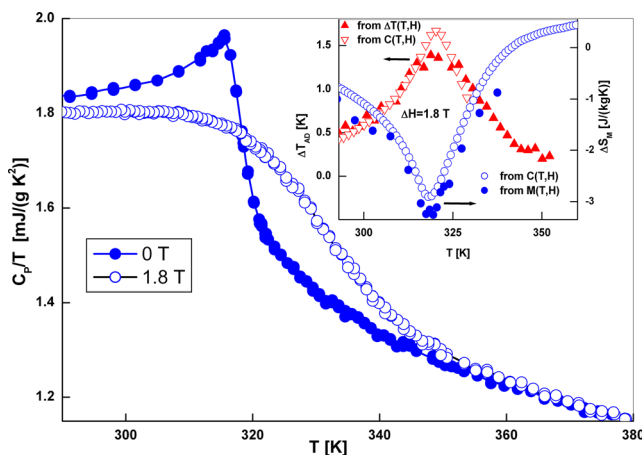


FIG. 4. The temperature dependencies of the specific heat capacity of $\text{Ni}_{50}\text{Mn}_{34.8}\text{In}_{14.2}\text{B}$ for zero and 1.8 T applied magnetic fields in the vicinity of T_C . Inset: adiabatic temperature changes obtained from direct $\Delta T(T,H)$ and indirect $C_p(T,H)$ measurements (left axis), and magnetic entropy changes from $C_p(T,H)$ and $M(T,H)$ measurements (right axis), in the vicinity of the magnetostructural phase transition for $\Delta H = 1.8$ T

$\Delta S(T, \Delta H)_T = S(T,H) - S(T,0)$.¹⁶ The adiabatic temperature change (ΔT_{AD}) has been determined from direct measurements and from $\Delta T(T,H)_S = T(S,H) - T(S,0)$.¹⁶ The results are in surprisingly good agreement (see the inset of Figure 4). For example, the value of ΔS_M estimated from the Clausius-Clapeyron equation following the procedure in Ref. 17 given as $\Delta S_M = -\Delta M(T_A)_{1.8T} \Delta H / \Delta T_A(\Delta H)$ was found to be (2.6-2.8) J/kgK for $\Delta H = 1.8$ T (see the inset of Fig. 2 for details), which is in excellent agreement with the ΔS_M calculated using the Maxwell relation for the $C(T,H)$ curves (see inset of Fig. 4).

It is worth mention that, in our case, ΔS_T is larger than ΔS_M ($H = 1.8$ T). These features indicate the following possible routes for MCE enhancement: (1) to use monocrystalline samples or polycrystalline samples with very sharp or nearly ideal MST's and (2) to find compounds with low-field-induced phase transformations. Obviously, there is still an opportunity for MCE enhancement in the $\text{Ni}_{50}\text{Mn}_{35}\text{In}_{15}$ based Heusler alloys because the theoretical limit $\Delta S_M = R \ln(2J + 1)$, where R is the universal gas constant and J is the average total angular moment per unit cell, is about 90 J/kgK, i.e., a value that is one order of magnitude larger than that observed in experiment.

The obtained values of $\Delta T_{AD} = 1.0$ K and $\Delta S_M = 1.5$ -2.0 J/kgK for $\Delta H = 1$ T are comparable to those reported for Gd, which is one of the most promising materials for room temperature refrigeration ($T_C = 293$ K, $\Delta T_{AD} \approx 2.5$ K per $\Delta H = 1$ T, $\Delta S \approx 2.5$ J/kgK for $\Delta H = 1$ T, and $C \approx 300$ J/kgK (Ref. 18)). It is worth to mention that the temperature interval (300-350 K) where quite large MCE was observed in these compounds is extremely important for possible refrigeration applications.

In summary, $\text{Ni}_{50}\text{Mn}_{34.8}\text{In}_{14.2}\text{B}$ exhibits a magnetostructural first order phase transition, from a ferromagnetic martensitic phase to a paramagnetic austenitic phase in the vicinity of 320 K, and is accompanied by a large MCE. The direct and indirect methods used to determine the MCE parameters are consistent with each other and are accurate. The MCE is large in the temperature range 300-350 K; the values of $\Delta T_{AD} = 1.0$ K and $\Delta S_M = 1.5$ -2.0 J/kgK for $\Delta H = 1$ T of $\text{Ni}_{50}\text{Mn}_{34.8}\text{In}_{14.2}\text{B}$ are comparable to that of Gd, which makes these types of compounds excellent prospects for future magnetic refrigeration devices.

¹T. Krenke, M. Acet, E. F. Wassermann, X. Moya, L. Mañosa, and A. Planes, *Phys. Rev. B* **73**, 174413 (2006).

²T. Krenke, E. Duman, M. Acet, E. Eberhard, F. Wassermann, X. Moya, L. Manosa, and A. Planes, *Phys. Rev. B* **75**, 104414 (2007).

³A. K. Pathak, M. Khan, I. Dubenko, S. Stadler, and N. Ali, *Appl. Phys. Lett.* **90**, 262504 (2007).

⁴X. Zhang, B. Zhang, S. Yu, Z. Liu, W. Xu, G. Liu, J. Chen, Z. Cao, and G. Wu, *Phys. Rev. B* **76**, 132403 (2007).

⁵I. Dubenko, M. Khan, A. K. Pathak, B. R. Gautam, S. Stadler, and N. Ali, *J. Magn. Magn. Mater.* **321**, 754 (2009).

⁶S. Y. Yu, Z. H. Liu, G. D. Liu, J. L. Chen, Z. X. Cao, G. H. Wu, B. Zhang, and X. X. Zhang, *Appl. Phys. Lett.* **89**, 162503 (2006).

⁷A. K. Pathak, I. Dubenko, Y. Xiong, P. W. Adams, S. Stadler, and N. Ali, *IEEE Trans. Mag.* **46**, 1444 (2010).

⁸I. Dubenko, A. K. Pathak, S. Stadler, N. Ali, Ya. Kovarskii, V. N. Prudnikov, N. S. Perov, and A. B. Granovsky, *Phys. Rev. B* **80**, 092408 (2009).

⁹A. K. Pathak, I. Dubenko, J. C. Mabon, S. Stadler, and N. Ali, *J. Phys. D: Appl. Phys.* **42**, 045004 (2009).

¹⁰B. R. Gautam, I. Dubenko, A. K. Pathak, S. Stadler, and N. Ali, *J. Phys.: Condens. Matter* **20**, 465209 (2008).

- ¹¹H. Luo, F. Meng, Q. Jiang, H. Liu, E. Liu, G. Wu, and Y. Wang, *Scr. Mater.* **63**, 569 (2010).
- ¹²H. C. Xuan, D. H. Wang, C. L. Zhang, Z. D. Han, and Y. W. Du, *Appl. Phys. Lett.* **92**, 102503 (2008).
- ¹³W. B. Pearson, *The Crystal Chemistry and Physics of Metals and Alloys* (Wiley-Interscience, New-York, 1972).
- ¹⁴M. Ye, A. Kimura, Y. Miura, M. Shirai, Y. T. Cui, K. Shimada, H. Namatame, M. Taniguchi, S. Ueda, K. Kobayashi, R. Kainuma, T. Shishido, K. Fukushima, and T. Kanomata, *Phys. Rev. Lett.* **104**, 176401 (2010).
- ¹⁵A. P. Kazakov, V. N. Prudnikov, A. B. Granovsky, A. P. Zhukov, J. Gonzalez, I. Dubenko, A. K. Pathak, S. Stadler, and N. Ali, *Appl. Phys. Lett.* **98**, 131911 (2011).
- ¹⁶K. A. Gschneidner, Jr., V. K. Pecharsky, and A. O. Tsokol, *Rep. Prog. Phys.* **68**, 1479 (2005).
- ¹⁷R. Kainuma, Y. Imano, W. Ito, Y. Sutou, H. Morito, S. Okamoto, O. Kitakami, K. Oikawa, A. Fujita, T. Kanomata, and K. Ishida, *Nature (London)* **439**, 957 (2006).
- ¹⁸S. Yu. Dan'kov, A. M. Tishin, V. K. Pecharsky, and K. A. Gschneidner, Jr., *Phys. Rev. B* **57**, 3478 (1998).